ATP-P2X7 Receptor Modulates Axon Initial Segment Composition and Function in Physiological Conditions and Brain Injury

Ana del Puerto, Laure Fronzaroli-Molinieres, María José Perez-Alvarez, Pierre Giraud, Edmond Carlier, Francisco Wandosell, Dominique Debanne, Juan José Garrido

Cerebral Cortex August 2015;25:2282–2294
doi:10.1093/cercor/bhu035
Advance Access publication March 7, 2014

ATP-P2X7 Receptor Modulates Axon Initial Segment Composition and Function in Physiological Conditions and Brain Injury

Ana del Puerto[1,2], Laure Fronzaroli-Molinieres[5,6], María José Perez-Alvarez[3], Pierre Giraud[5,6], Edmond Carlier[5,6], Francisco Wandosell[2,4], Dominique Debanne[5,6] and Juan José Garrido[1,2]

[1]Instituto Cajal, CSIC, Department of Cellular, Molecular and Developmental Neurobiology, Madrid 28002, Spain, [2]Centro de Investigación Biomédica en Red Sobre Enfermedades Neurodegenerativas (CIBERNED), Madrid, Spain, [3]Departamento de Biología (Unidad Docente Fisiología Animal), Universidad Autónoma de Madrid, Madrid 28049, Spain, [4]Centro de Biología Molecular, CSIC-UAM, Madrid 28049 Spain, [5]Institut National de la Santé et de la Recherche Médicale, U1072, Marseille F-13344 France and [6]Aix-Marseille Université, Faculté de Médecine Secteur Nord, Marseille F-13344 France

Address correspondence to Juan José Garrido, PhD, Instituto Cajal, CSIC, Avenida Doctor Arce, 37, Madrid 28002, Spain.
Email: jjgarrido@cajal.csic.es

Axon properties, including action potential initiation and modulation, depend on both AIS integrity and the regulation of ion channel expression in the AIS. Alteration of the axon initial segment (AIS) has been implicated in neurodegenerative, psychiatric, and brain trauma diseases, thus identification of the physiological mechanisms that regulate the AIS is required to understand and circumvent AIS alterations in pathological conditions. Here, we show that the purinergic P2X7 receptor and its agonist, adenosine triphosphate (ATP), modulate both structural proteins and ion channel density at the AIS in cultured neurons and brain slices. In cultured hippocampal neurons, an increment of extracellular ATP concentration or P2X7-green fluorescent protein (GFP) expression reduced the density of ankyrin G and voltage-gated sodium channels at the AIS. This effect is mediated by P2X7-regulated calcium influx and calpain activation, and impaired by P2X7 inhibition with Brilliant Blue G (BBG), or P2X7 suppression. Electrophysiological studies in brain slices showed that P2X7-GFP transfection decreased both sodium current amplitude and intrinsic neuronal excitability, while P2X7 inhibition had the opposite effect. Finally, inhibition of P2X7 with BBG prevented AIS disruption after ischemia/reperfusion in rats. In conclusion, our study demonstrates an involvement of P2X7 receptors in the regulation of AIS mediated neuronal excitability in physiological and pathological conditions.

Keywords: ankyrin G, axon initial segment, BBG, brain ischemia, P2X7 receptor, sodium channels

Introduction

The axon initial segment (AIS) is not only the locus of action potential initiation (Kole et al. 2008) but it also plays an essential role in maintaining axon integrity and identity (Hedstrom et al. 2008). The property of spike initiation is conferred by the high concentration of voltage-gated ion channels in the AIS (Bender and Trussell 2012) maintained by cytoskeletal proteins, such as ankyrin G or PSD-93 (Garrido et al. 2003; Pan et al. 2006; Ogawa et al. 2008). The cellular and molecular machinery that finely modulates functional expression of ion channels at the AIS remains mostly unknown. Recent studies have shown that kinases in the AIS (i.e., Casein kinase 2, GSK-3, and cdk5) can modulate the density of AIS proteins (Brechet et al. 2008; Sanchez-Ponce et al. 2011; Vacher et al. 2011; Tapia et al. 2013). Moreover, neuronal excitability is also controlled in certain neuronal types through modifications of the position and length of the AIS (Grubb and Burrone 2010; Kuba et al. 2010). This AIS plasticity is controlled at least by the influx of calcium through T- and/or L-type voltage-gated calcium channels or metabotropic glutamate receptors and higher physiological $[Ca^{2+}]_i$, that modulate calcineurin activity (Evans et al. 2013). Besides physiological regulation of the AIS, AIS alterations have been reported in neurological disorders and nervous system injury (Buffington and Rasband 2011). In this context, some neurological disorders, such as Angelman syndrome or schizophrenia; or brain trauma are related to structural alterations of the AIS or changes in the expression of structural proteins and ion channels in the AIS (Cruz et al. 2009; Kaphzan et al. 2011; Baalman et al. 2013; Hinman et al. 2013). Moreover, AIS is disrupted after brain ischemia by a calcium/calpain-dependent mechanism, independent of *N*-methyl-D-aspartate (NMDA) receptor activation (Schafer et al. 2009). In this sense, P2X purinergic receptors are good candidates to control calcium influx in physiological and pathological conditions.

Seven P2X receptors have been cloned (P2X1-7). They are all expressed in neurons and glial cells during brain development and in adult brain. These receptors are activated by extracellular adenosine 5′-triphosphate (ATP) and allow calcium influx to the same extent as NMDA receptors (Abbracchio et al. 2009). Among the 7 P2X purinergic receptors, P2X7 is the one that needs higher ATP concentrations (>100 μM) for its activation (North and Surprenant 2000). In addition, it has been proposed that P2X7 receptor triggers quantal release of ATP (Gutierrez-Martin et al. 2011). P2X7 receptor stimulation has been implicated in several nervous system diseases, such as brain ischemia, epileptic seizures, multiple sclerosis, spinal cord injury, Alzheimer''s disease, or Huntington's disease (Vianna et al. 2002; Parvathenani et al. 2003; Wang et al. 2004; Matute et al. 2007; Diaz-Hernandez et al. 2009; Kim et al. 2009; Arbeloa et al. 2012). Furthermore, recent studies have shown that suppression or inhibition of P2X7 receptor promotes axonal growth, suggesting a role of their antagonists in axonal regeneration and axonal physiology (Diaz-Hernandez et al. 2008; del Puerto et al. 2012).

Our study demonstrates that an increase in the extracellular ATP concentration reduces the density of βIV-spectrin, ankyrin G, and voltage-gated sodium channels at the AIS, via a process that depends on P2X7 activity, calcium, and calpain. In this sense, we show that AIS disruption observed after brain ischemia is prevented by a P2X7 receptor antagonist. Finally,

electrophysiological studies in brain slices show P2X7 involvement in the modulation of sodium currents, action potential generation and neuronal excitability. Thus, our study suggests a new role for purines and ATP-gated P2X7 purinergic receptors in the regulation of the AIS.

Materials and Methods

Reagents and Plasmids

ATP (A5394), Brilliant Blue G (BBG, B0770) and ethyleneglycol-bis (2-aminoethylether)-*N*,*N*,*N*′,*N*′-tetra acetic acid (EGTA) (E3889) were obtained from Sigma-Aldrich, Calpeptin was from Calbiochem (03340051) and MDL-28170 from Tocris (1146). GFP plasmid was obtained from Clontech, P2X7-GFP, P2X7 interference RNA and scrambled RNA plasmids used in this study have been used and described in previous publications (Diaz-Hernandez et al. 2008; del Puerto et al. 2012).

Animals

Animals were housed in a room at controlled temperature and relative humidity with alternating 12 h light and dark cycles and free access to food and water "ad libitum". Animal care protocols used in our laboratory are in conformity with the appropriate national legislation (53/2013, BOE no. 1337), and guidelines of the Council of the European Communities (2010/63/UE). All protocols were previously approved by CSIC bioethics committee.

Induction of Transient Focal Cerebral Ischemia (tMCAO)

Fifteen adult male Wistar rats ~8 weeks old (250–310 g) obtained from CBM animal facilities were used for the study. Transient focal cerebral ischemia was induced using the intraluminal suture method by the middle cerebral artery occlusion (MCAO) procedure as described previously (Longa et al. 1989). Rats were anesthetized under isoflurane (3% for induction and 1–1.5% for maintenance) delivered via a face mask in oxygen-enriched air. The right common carotid artery (CCA) was exposed and dissected; the right external carotid artery (ECA) and the right internal carotid artery (ICA) were isolated. The first artery branches of the ECA and the pterygopalatine artery were electrocauterized using a High Temperature Cautery Power Handle (Aaron Medical, Clearwater, USA). A 4-0 monofilament nylon suture Dafilon (B. Braun, Tuttlingen, Germany) with its tip rounded by heating and poly-L-lysine coated, was introduced into the ECA lumen and advanced into the ICA lumen until a mild resistance was felt, ~2.2 cm beyond the CCA bifurcation to occlude the origins of the middle cerebral artery (MCA). The suture was secured in place with a ligature and was maintained for 90 min. After this time the suture was removed thus allowing tissue reperfusion. The sham operated rats received all surgical procedures but without the suture insertion. All animals received ibuprofen (Dalsy, Abbot) as an analgesic, diluted at 200 mg/L in the drinking water for 48 h after surgery. Some rats (sham and tMCAO) were treated with 5 doses of BBG (50 mg/kg), by intraperitoneal injection at 3 and 6 h after reperfusion and then twice a day. All the animals were sacrificed after 72 h of the onset of ischemia.

Neurologic Deficit Score

The neurological deficit score of each rat was measured before surgery, during the first 6 h after tMCAO induction and just before administration of BGG, using a slightly modified version of the method described by Yrjanheikki et al. (2005). The neurological deficit score of each rat was performed to check whether ischemia was correctly induced and before each injection. A 6-point neuroscore test of the motor status was recorded. Rats were scored 5 when both forelimbs showed a normal extension towards the floor when lifted; 4 in the case of dysfunctional rats with consistently reduced resistance to lateral push towards the paretic side; 3 when rats did circle towards the paretic side if pulled and lifted by the tail; 2 if circling towards the paretic side when pulled by the tail; 1 when circling towards the paretic side spontaneously and 0 if no spontaneous motion. Additionally the animals were evaluated for any other neurological abnormalities that had not been included in the previous grade scale, such as keeping their balance, sensorial perception (acoustic, visual localization), and reflexes (corneal, palpebral, postural correction). Only ischemic animals that showed a neurological score of 3 or lower during the first 6 h after ischemia induction were included in the study.

Tissue Collection

After 72 h of the onset of ischemia, the rats were sacrificed by deep anesthesia by intraperitoneal injection of a mixture of medetomidine (375 μg/kg) and ketamine (112.5 mg/kg). Deeply anesthetized animals were transcardially perfused with ice-cold phosphate-buffered saline (PBS) and then with 4% paraformaldehyde in 0.1 M phosphate buffer (pH 7.4). Brains were removed and postfixed 1 h at 4°C. Subsequently, the brains were washed 3 times in PBS (15 min each), and cryoprotected in 30% sucrose in PBS at 4°C for 48–72 h. Finally, the brains were embedded in Tissue-Tek medium (Sakura, Zoeterwoude, NL) and stored at −20°C until used. Coronal cryostat sections (30-μm thick) were obtained from each brain and sections located from +2 to −2 relative to the bregma were selected for immunochemistry experiments.

Neuronal Culture

Mouse hippocampal neurons were prepared as previously described (Kaech and Banker 2006). Neurons were obtained from E17 mouse hippocampi, which were incubated in a 0.25% trypsin solution in Ca^{2+}/Mg^{2+} free Hank's buffered salt solution (HBSS) and dissociated using fire polished Pasteur pipettes. The cells were plated on polylysine-coated coverslips (1 mg/mL) at a density of 5000 cells/cm^2 for 2 h in plating medium (minimum essential medium [MEM], 10% horse serum, 0.6% glucose, Glutamax-I and antibiotics). Then, coverslips were inverted and transferred to culture dishes containing astrocytes. Astrocytes medium was replaced by neuronal culture medium 24 h before (Neurobasal medium, B27 supplement, Glutamax-I). To avoid contact between neurons and astrocytes paraffin beads were placed on coverslips before neuronal plating. 5 μM 1-β-D-arabinofuranosylcytosine (AraC) was added after 2 days in culture to avoid glial proliferation. Primary hippocampal neurons were nucleofected using the Amaxa nucleofector kit for primary mammalian neural cells (Amaxa Bioscience) according to the manufacturer's instructions. Nucleofection was performed using 3 μg total DNA and 3×10^6 cells for each nucleofection. Nucleofection efficiency was ~15% of neurons, based on the number of GFP positive neurons.

Immunofluorescence

Coverslips were treated for 10 min with 50 mM NH_4Cl and incubated in blocking buffer (0.22% gelatin, 0.1% Triton X-100 in PBS) for 30 min, before incubation with primary antibodies for 1 h at room temperature in blocking buffer. Brain sections were incubated in blocking buffer (10% goat serum, Triton X-100 0.5% in PBS) for 1 h before overnight incubation with primary antibodies in the same buffer. The primary antibodies used were: chicken anti-MAP2 (1:10 000, Abcam), mouse anti-PanNaCh (1:75, Sigma), mouse antiankyrin G (1:100) from NeuroMab. Rabbit anti βIV-spectrin (1:500), kindly provided by Dr Matthew Rasband (Baylor College, Houston). The secondary antibodies used were a donkey antimouse, antirabbit, or antichicken Alexa-Fluor-488, 594, or 647 (1:500). Nuclei were stained using 4′,6-diamidino-2-phenylindole, and coverslips were mounted in Fluromount G. Images were acquired on a vertical Axioskop-2plus microscope (Zeiss) or a confocal microscope (LSM510, Zeiss) under the same conditions to compare intensities. Figures were prepared for presentation using the Adobe CS3 software. Quantification of fluorescence intensity at the AIS was performed in 150 neurons per experimental condition in 3 independent experiments. Measurements of AIS proteins location and intensity in immunocytochemistry experiments were performed with confocal images using MatLab script according to Grubb and Burrone (2010). Briefly, image stacks were converted into single maximum intensity *z*-axis projections, exported as raw 16-bit TIFF files, and imported into Matlab (Mathworks) for analysis using MatLab script.

We drew a line profile starting at the soma that extended through the axon, past the AIS. At each pixel along this profile, fluorescence intensity values were averaged over a 3 × 3 pixel square centered on the pixel of interest. Averaged profiles were then smoothed and normalized between 1 (maximum smoothed fluorescence, location of the AIS max position) and 0 (minimum smoothed fluorescence) and finally were normalized to the mean control value in each experiment. AIS start and end positions were obtained at the proximal and distal axonal positions, respectively, where the normalized profile declined to 0.33.

Hippocampal Slices Cultures and Biolistic Transfection

Slice cultures containing the hippocampus and entorhinal cortex were obtained from postnatal day 7 mice as previously reported (Debanne et al. 2008). Slices (350–450 µm) were cut in sucrose-based slicing solution (280 mM sucrose, 26 mM $NaHCO_3$, 1.3 mM KCl, 1 mM $CaCl_2$, 10 mM $MgCl_2$, 11 mM D-glucose, 50 mM phenol red, and 2 mM kynurenate) and were maintained for 1 h at room temperature in oxygenated (95% O_2/5% CO_2) standard artificial cerebrospinal fluid (125 mM NaCl, 2.5 mM KCl, 0.8 mM NaH_2PO_4, 26 mM $NaHCO_3$, 3 mM $CaCl_2$, 2 mM $MgCl_2$, 50 mM phenol red, and 11 mM D-glucose). Each slice was placed on 20-mm latex membranes (Millicell) inserted into 35-mm Petri dishes containing 1 mL of culture medium (25 mL MEM, 12.5 mL HBSS, 12.5 mL horse serum, 0.5 mL penicillin/streptomycin, 0.8 mL glucose solution (1 M), 0.1 mL ascorbic acid solution (1 mg/mL), 0.4 mL 4-(2-hydroxyethyl)-1-piperazineethanesulfonic acid (HEPES) (1 M), 0.5 mL B27, and 8.95 mL water) and kept at 34°C, 95% O_2–5% CO_2. To arrest glial proliferation, 5 µM Ara-C was added to the culture medium. BBG treatment carried out at a concentration of 200 nM the next day and kept for 2 days before electrophysiological experiments. For transfection experiments, GFP or P2X7-GFP plasmids were delivered to brain slices using the Helyos gene-gun system (Bio-Rad) according to the manufacturer's instructions. Briefly, gold particles covered with each plasmid were delivered at a pressure of 100 dpi into brain slices cultured for 2 days, and then brain slices were kept for a further 48 h before electrophysiological recording or fixation for immunohistochemistry. Slices were fixed for immunohistochemistry using 4% PFA for 1 h and washed in PBS. Slices were incubated overnight with primary antibody: rabbit anti-βIV-spectrin; in PBS containing 20% goat serum and 0.5% Triton X-100. Secondary antibody was incubated for 4 h before mounting brain slices in Fluoromount G. Confocal images were acquired on a Leica TCS SP2 laser scanning microscope (Leica Microsystems).

Electrophysiological Studies

Whole-cell patch clamp recordings were obtained from CA3 or L5 pyramidal neurons. The external solution contained (mM): 125 NaCl, 26 $NaHCO_3$, 3 $CaCl_2$, 2.5 KCl, 2 $MgCl_2$, 0.8 NaH_2PO_4, and 10 D-glucose, and was equilibrated with 95% O_2–CO_2. Patch pipettes (5–10 MΩ) were filled with a solution containing (mM): 120 potassium gluconate, 20 KCl, 0.5 EGTA, 10 HEPES, 2 Na_2ATP, 0.3 NaGTP and 2 $MgCl_2$, pH 7.4. Recordings were made at 29°C. The voltage and current signals were low-pass filtered (3 kHz) and acquisition of sequences (500–1.500 ms) was performed at a frequency of 0.1 Hz with P-clamp 8 or 10 (Axon Instruments). Sodium currents were evoked by a voltage step (50 ms) from −70 to 0 mV. The capacitive and leak components of the evoked current were subtracted with a conventional P/4 protocol. Intrinsic neuronal excitability was monitored with depolarizing current pulses (1 s) of increasing amplitude (from +10/+500 pA).

Statistical Analysis

Statistical analysis was carried out in Sigmaplot v11 (Systat Software Inc.). Data for each independent sample were obtained from at least 3 independent experiments. Data from each experiment were collected from at least 50 cells (between 50 and 80 cells) in each experimental sample. We compared the data from each 2 experimental samples using a *t*-test. Before carrying out the test, Sigmaplot software did check for normal distribution of data. Some data sets failed the normality test (Shapiro–Wilk test). For that reason, we used a nonparametric Mann–Whitney *U*-test for all 2 independent sample comparisons (data in Figs 1–5). All tests were 2-tailed. Differences were considered significant when $P < 0.05$. Electrophysiological data were compared using a *t*-test.

Results

P2X7 Activity Modulates AIS Structure and Protein Composition

Calcium is an important regulator of AIS function and is also involved in AIS disruption in brain ischemia. However, AIS disruption is not rescued after ischemia by an NMDA antagonist (Schafer et al. 2009). As mentioned above, P2X7 receptor allows calcium influx to the same extent as NMDA receptors. In order to analyze whether P2X7 receptors are involved in the regulation of the AIS, we treated 20 DIV hippocampal neurons with ATP, the P2X7 receptor agonist, increasing the concentration of ATP in the extracellular medium (+1 mM) for 24 h. ATP treatment significantly reduced the concentration of ankyrin G at the AIS (Fig. 1*A*,*C*), sparing only 62.3 ± 2.7% of the fluorescence observed in control neurons (100%). This reduction was observed all along the AIS (Fig. 1*D*), without any change in AIS length or position (Supplementary Fig. 1). Similar results were obtained for voltage-gated sodium channels (PanNaCh), 70.6 ± 4.7% compared with control neurons (Fig. 1*B*,*E*). Interestingly, cotreatment with ATP (+ 1 mM) and BBG (100 nM) for 24 h not only prevented this reduction but significantly increased ankyrin G (111.4 ± 3.9%, Fig. 1*A*,*C*) and PanNaCh (118.1% ± 7.1%) staining (Fig. 1*B*,*E*). BBG treatment alone also increased the density of AIS proteins (Fig. 1*A*–*D*). Hence, inhibition of P2X7 receptors prevents the loss of AIS proteins produced by elevated extracellular ATP.

We then asked whether BBG-mediated P2X7 receptor inhibition could rescue the loss of AIS proteins induced by ATP treatment. Thus, neurons previously exposed to ATP (+1 mM) for 21 h were treated with increasing concentrations of BBG (10 , 50, and 100 nM) for 3 additional hours maintaining ATP treatment (Fig. 2*A*). In these experimental conditions, concentrations of 50 nM BBG or higher rescued ankyrin G staining at the AIS from 60.5 ± 2.5% in ATP treated neurons to 128.5 ± 5.4% (ATP + BBG 50 nM) or 98.1 ± 3.6% (ATP + BBG 100 nM) compared with 100% in control neurons (Fig. 2*A*–*C*). Similar results were obtained for voltage-gated sodium channels (Fig. 2*D*,*E*). This result confirms a role of the P2X7 receptor in modulating density of AIS proteins.

In view of these results and to further substantiate the role of P2X7, hippocampal neurons were nucleofected, before plating, with plasmids expressing GFP or P2X7-GFP, and plasmids that coexpress P2X7 interference RNA (sh P2X7) or its corresponding scrambled interference RNA (sc shRNA) and GFP. Neurons were maintained 20 DIV and treated with BBG (100 nM) or ATP (+1 mM) in different experimental conditions. AISs of neurons expressing P2X7-GFP receptor displayed only the 60.4 ± 4.1% and 67.3 ± 4.3% of the fluorescence quantified in GFP-nucleofected neurons for ankyrin G or sodium channel, respectively (Fig. 3*A*,*C*,*D*). Ankyrin G and sodium channel fluorescence in GFP-nucleofected neurons was equal to that observed in surrounding nonnucleofected neurons. This reduction of AIS proteins produced by P2X7-GFP expression was prevented, and expression was even increased, by combined treatment with BBG for the last 24 h (116 ± 6.8%, PanNaCh and 124.7 ± 9.4%, ankyrin G), as previously shown

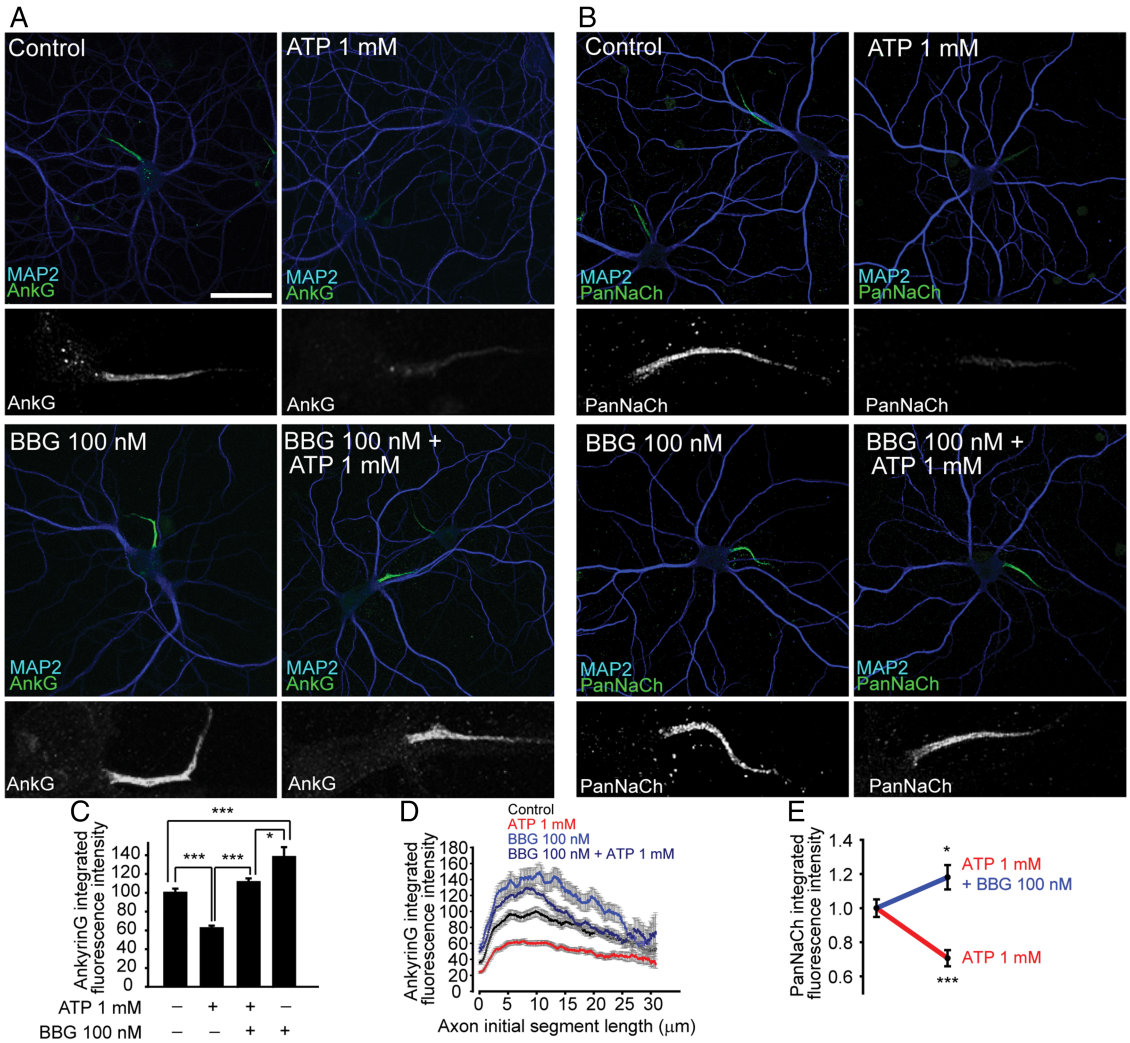

Figure 1. P2X7 receptor activation reduced the density of ankyrin G and voltage-gated sodium channels at the AIS (*A*,*B*) Hippocampal neurons were cultured for 20 DIV and then treated for 24 h with 1 mM ATP, 100 nM BBG or the combination of both. Neurons were fixed and stained with anti-MAP2 antibody (blue) and antiankyrin G (A) or PanNaCh (B) antibodies (green). The ×4 magnifications of AIS staining are shown under each image. Scale bar = 50 μm. Images of each experimental condition from 3 independent experiments obtained under the same conditions. Ankyrin G and PanNaCh fluorescence intensity were measured using Matlab software. (*C*) Quantification of total integrated ankyrin G fluorescence intensity. (*D*) Quantification of ankyrin G fluorescence intensity along the AIS. (*E*) Quantification of total integrated PanNaCh fluorescence intensity. All quantifications were done in at least 50 neurons in each experimental condition and experiment. Data are represented as the mean ± SEM of at least 3 independent experiments. Individual data were normalized to the control mean. (*$P < 0.05$; ***$P < 0.001$, Mann–Whitney test).

for BBG in experiments where neurons were treated with the P2X7 agonist ATP (Fig. 1*A*,*C*,*D*). Next, we nucleofected neurons with P2X7 interference RNA or scrambled interference RNA to analyze the effect of ATP on AIS proteins in neurons with reduced P2X7 function. The expression of P2X7 interference RNA significantly increased the expression of ankyrin G (135.7 ± 11.5%), indicating a role for P2X7 in the downregulation of AIS protein tethering at the AIS. This fact was confirmed when neurons expressing P2X7 interference RNA were treated with ATP. While neurons that were non-nucleofected or nucleofected with scrambled interference RNA showed a decreased AIS protein staining (75.9% ± 4.7%), those with reduced P2X7 expression were not affected by ATP treatment, and ankyrin G and sodium channels staining at the AIS was similar to control neurons in the absence of ATP treatment, 113.9 ± 10.4% and 116.2 ± 9.8%, respectively. (Fig. 3*B*,*E*,*F*).

These data demonstrate a role for P2X7 and extracellular ATP in the regulation of AIS proteins, which then raises the question as to the molecular mechanisms modulated by P2X7 that regulate the tethering and maintenance of proteins at the AIS?

P2X7 Modulation of AIS Proteins is Mediated by Calcium and Calpain

Activation of P2X7 by ATP triggers calcium influx and increased intracellular calcium concentration. Calcium entry is mediated directly by P2X7 purinoreceptor, but also by indirect opening of voltage-dependent calcium channels to further increase $[Ca^{2+}]_i$. Studies in NG108-15 cells demonstrate that at least 31% of ATP-mediated calcium influx is not prevented by a combination of voltage-dependent calcium channels blockers (Brater et al. 1999), which in contrast prevents completely the KCl mediated intracellular calcium increase. Thus, we first checked the effect of increased extracellular calcium concentration on the AIS. The extracellular calcium concentration was

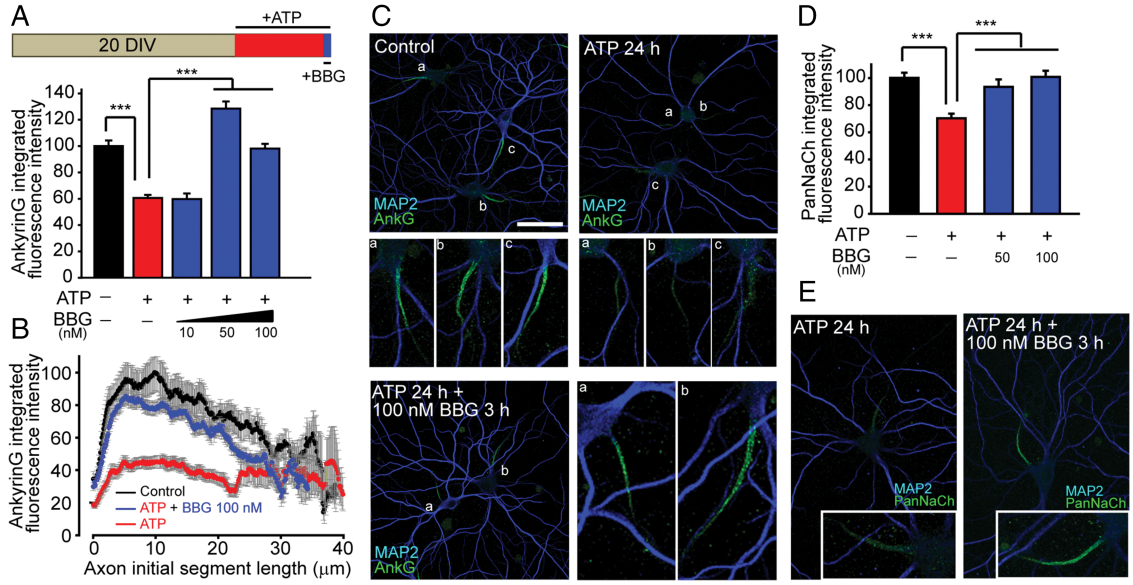

Figure 2. The P2X7 receptor antagonist BBG rescued ankyrin G and sodium channel density at the AIS after ATP treatment. Hippocampal neurons were cultured for 20 DIV before treatment with ATP for 24 h. BBG was added for the last 3 h of treatment at increasing concentrations from 10 to 100 nM. Neurons were fixed and stained with antibodies against ankyrin G (green) or sodium channels (PanNaCh, green) and MAP2 (blue). (*A*) Quantification of total integrated ankyrin G fluorescence intensity. Data are represented as the mean ± SEM of 3 independent experiments (*B*) Mean ± SEM ankyrin G fluorescence intensity along the AIS of 3 experiments. (*C*) Representative images and ×4 magnifications of control and treated neurons stained with antiankyrin G antibody (green) and MAP2 (blue). Axons initial segments in each figure are identified by letters and the corresponding magnification is shown at the bottom of each image. Scale bar = 50 μm. (*D*) Quantification of integrated sodium channel fluorescence intensity at the AIS. Data are represented as the mean ± SEM of 3 independent experiments. (*E*) Representative images and ×4 magnifications of control and treated neurons stained with antiPanNaCh antibody (green) and MAP2 (blue). All quantifications were done in at least 50 neurons in each experimental and experiment. Individual data were normalized to the control mean. (***$P < 0.001$, Mann–Whitney test).

increased by adding 2 mM or 5 mM $CaCl_2$ to the culture medium of 20 DIV hippocampal neurons for 24 h. Both treatments reduced the density of ankyrin G at the AIS (62.7 ± 3.2%, 2 mM and 27.4 ± 2.6%, 5 mM). In the same experiments, cotreatment with 100 nM BBG impaired the reduction observed with 2 mM $CaCl_2$ (117.7% ± 6%), indicating that the effect of calcium was mediated by the P2X7 receptor (Fig. 4*A*,*B*). Then, we analyzed whether decreasing the extracellular calcium concentration with EGTA prevented the ATP-mediated reduction of ankyrin G. In fact, treatment of neurons for 24 h with ATP in the presence of 2 mM EGTA preserved ankyrin G levels (89.8 ± 6.2% vs. 58.2 ± 2.8% in ATP treated neurons) (Fig. 4*B*). Similar results were obtained for voltage-gated sodium channels (Fig. 4*C*,*F*), for which expression at the AIS was reduced by increased extracellular calcium concentration and ATP, and stabilized by EGTA or BBG. These data were confirmed in neurons expressing P2X7-GFP or P2X7 interference RNA. The addition of 2 mM $CaCl_2$ to the medium failed to decrease ankyrin G levels in neurons when P2X7 receptor expression was reduced by interference RNA (100.1 ± 10.9% vs. 50.1 ± 3.4% in scrambled shRNA nucleofected neurons; Fig. 4*D*), demonstrating that calcium mediated reduction of AIS proteins depends on P2X7. In a similar way, sequestering extracellular calcium with 2 mM EGTA blocked the reduction in the concentration of AIS proteins mediated by P2X7-GFP (109.7 ± 6.8% vs. 63.6 ± 3.7% for ankyrin G and 99.4 ± 7.7% vs. 67.8 ± 4.3% for PanNaCh; Fig. 4*D*,*E*,*G*). Once a role for calcium and P2X7 in AIS regulation was confirmed and taking into account that the inhibition of calpain, a calcium-activated protease, prevents AIS injury (Schafer et al. 2009), we analyzed whether 2 calpain inhibitors (calpeptin and MDL) could prevent the decrease in AIS proteins mediated by ATP and P2X7 (Fig. 5). Hippocampal neurons at 20 DIV were treated with 1 mM ATP in the presence or absence of 10 μM calpeptin or 50 nM MDL for 24 h. The ATP-induced reduction of ankyrin G and sodium channel staining was prevented by both calpain inhibitors (Fig. 5*A*–*C*). Similar results were obtained in neurons expressing P2X7-GFP (Fig. 5*D*–*F*), where calpeptin and MDL blocked the reduction in ankyrin G and sodium channel density, maintaining levels similar to those of nonnucleofected neurons (Fig. 5*D*).

P2X7 Receptors Modulate Voltage-gated Sodium Currents and Neuronal Excitability

All these data suggest that changes in P2X7 receptor activity are important for the regulation of voltage-gated ion channels at the AIS, implicating this receptor in the modulation of neuronal excitability. To corroborate the data obtained in hippocampal cultured neurons and consolidate this latter hypothesis, hippocampal slice cultures containing the entorhinal cortex were used. Slices were treated with the P2X7 antagonist, BBG and kept in culture for at least 48 h before testing the electrophysiological properties of the neurons (Fig. 6). CA3 pyramidal neurons treated with BBG (200 nM) for 48 h, displayed an enhanced sodium current (148.5 ± 13.8%) compared with control neurons (100 ± 9.9%, Fig. 6*A*). Then, we analyzed in current clamp whether neuronal excitability and action potential number was altered by the P2X7 antagonist. Consistent with voltage clamp recordings, BBG increased the number of action potentials (Fig. 6*B*).

To consolidate the role of P2X7 receptors in regulating sodium current and neuronal excitability, we expressed P2X7-GFP receptors in brain slices using the GeneGun

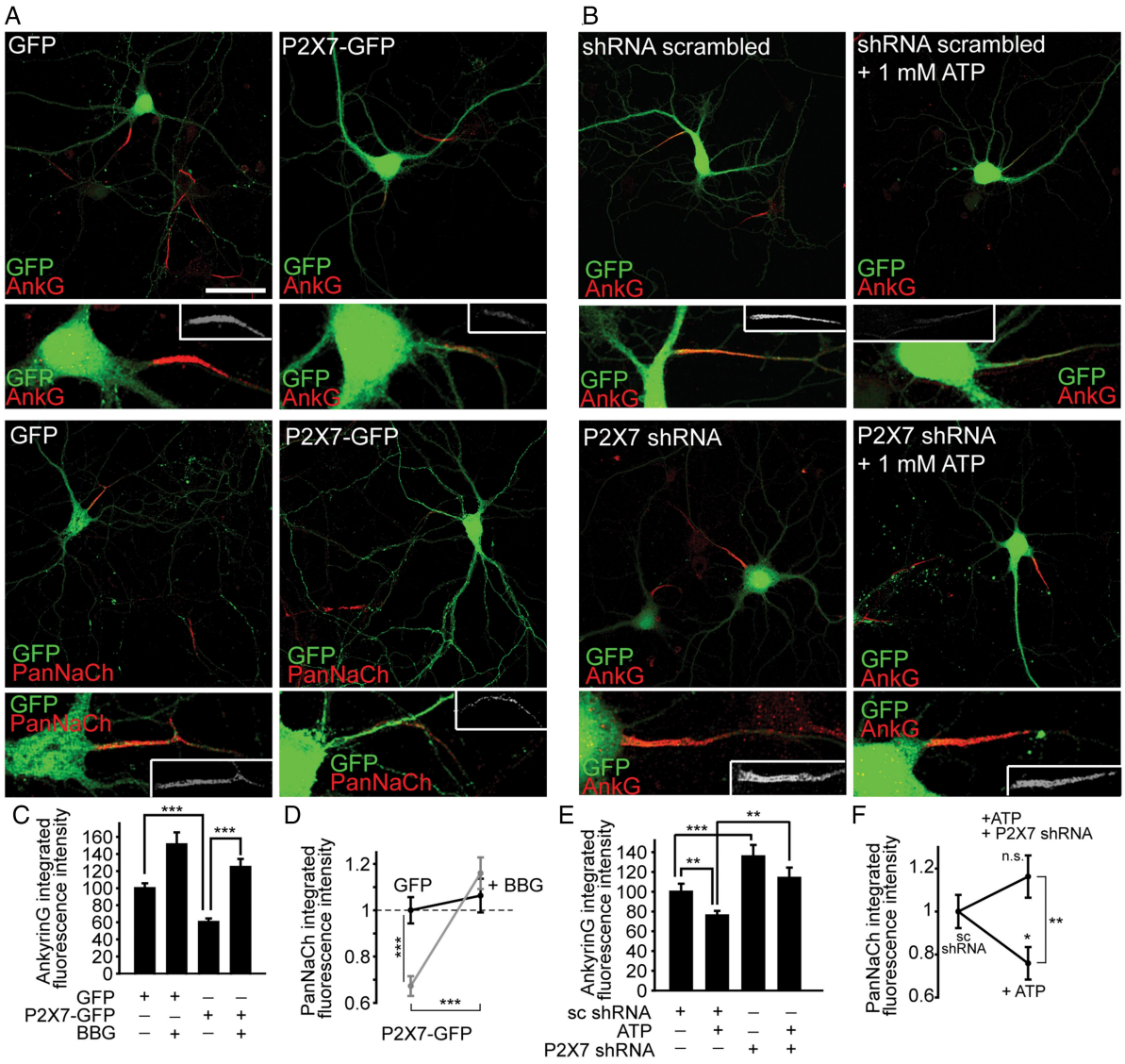

Figure 3. Effects of expression of P2X7 receptor-GFP or P2X7 receptor interference RNA on AIS protein density. Hippocampal neurons were nucleofected with plasmids expressing GFP or P2X7-GFP (*A*) and scrambled interference RNA or P2X7 interference RNA (*B*) and maintained in culture for 20 DIV before treatment with BBG or ATP for 24 h. Neurons were fixed and stained with antibodies against ankyrin G or PanNaCh (red). Nucleofected neurons were identified by GFP expression (green). The ×4 magnifications of AISs from nucleofected neurons are shown under each image. Scale bar = 50 μm. (*C*,*E*) Quantification of integrated ankyrin G fluorescence intensity at the AIS. (*D*,*F*) Quantification of integrated PanNaCh fluorescence intensity. All quantifications were done in at least 50 neurons in each experimental and experiment. Data are represented as the mean ± SEM of at least 3 independent experiments. Individual data were normalized to the control mean. (n.s.: nonsignificant; $^{*}P < 0.05$; $^{**}P < 0.01$; $^{***}P < 0.001$, Mann–Whitney test).

technique, and due to the low number of hippocampal neurons transfected, we decided to analyze layer 5 pyramidal cortical neurons (Fig. 7). Electrophysiological recordings were made in neurons expressing P2X7-GFP and nearby control neurons to minimize possible variability due to culture conditions or to shot gold particles. Previous studies have shown that GFP expression do not affect neither resting membrane potential, membrane conductance, actions potentials, nor firing accommodation (Ehrengruber et al. 2001). To confirm that P2X7-GFP expression was affecting AIS in brain slices, some slices were fixed and stained with an AIS marker (βIV-spectrin antibody). In P2X7-GFP positive neurons, βIV-spectrin staining was absent or much reduced at the AIS, compared with surrounding nontransfected neurons, or neurons transfected with GFP or P2X7 interference RNA (Fig. 7*A*,*B*). Confirming the reduction of sodium channel density at the AIS of cultured neurons treated with ATP, layer 5 cortical neurons expressing P2X7-GFP had a diminished sodium current amplitude (383.2 ± 67.5 pA/pF) vs. nearby control neurons (697.6 ± 117.8 pA/pF) (Fig. 7*C*). In addition, P2X7-GFP positive neurons showed a significant reduction in the number of action potentials and a higher current threshold for the generation of action potentials (Fig. 7*D*,*E*).

P2X7 Antagonism Prevents Injury of the AIS After Brain Ischemia

Our results demonstrate a role of P2X7 receptor and calcium in AIS modulation. Next, we checked whether the calcium-permeable ATP-gated P2X7 receptor could impair AIS disruption or play a role in AIS modulation in brain ischemia. Transient ischemia was induced by MCAO in 6 rats for 90 min before

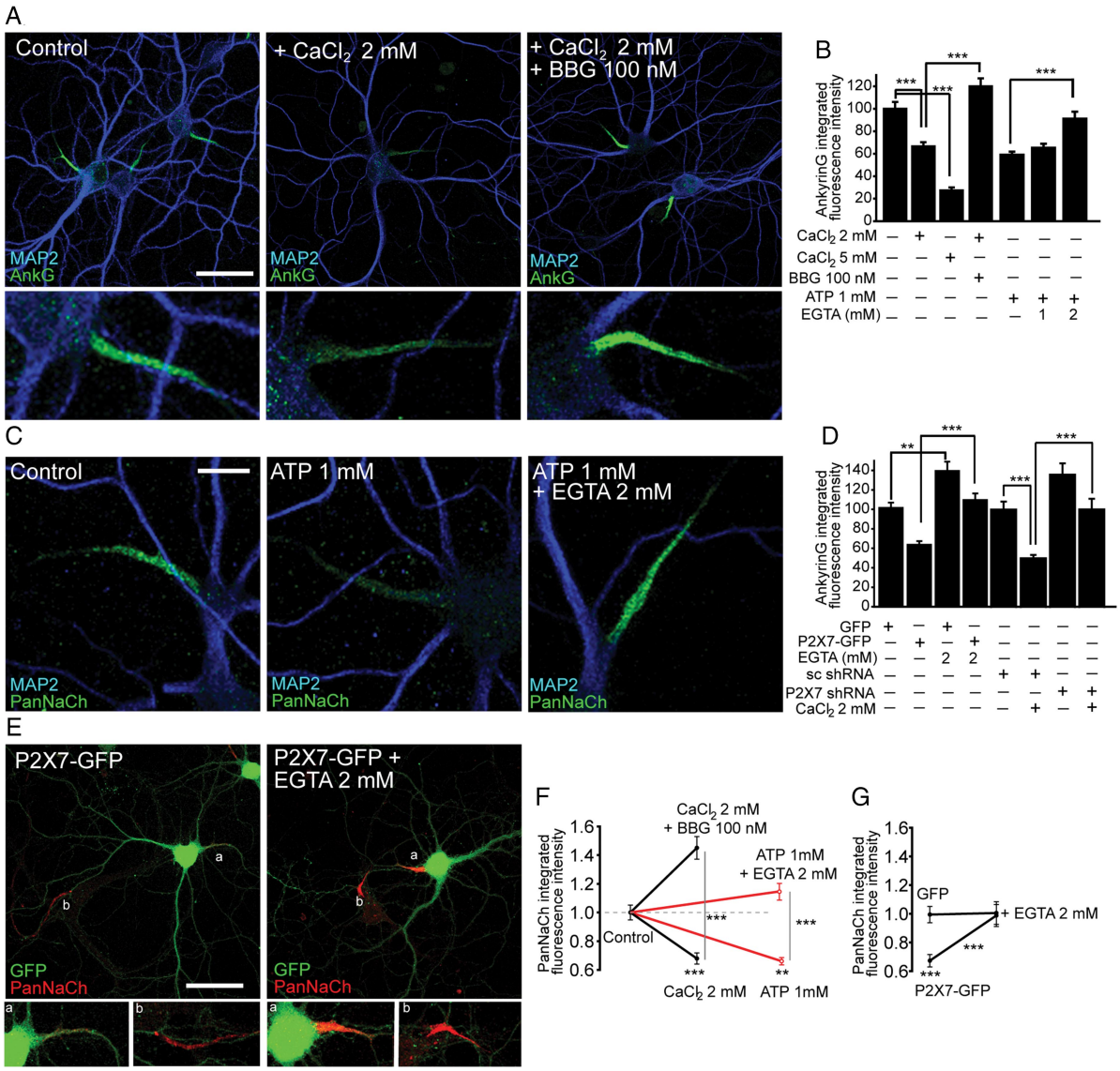

Figure 4. P2X7 receptor-dependent calcium influx mediates the reduction in AIS protein density. (*A*) Hippocampal neurons were cultured for 20 days and then calcium concentration was increased by adding $CaCl_2$ (+2 mM) for 24 h in the presence or absence of 100 nM BBG. Neurons were fixed, stained with antiankyrin G antibody (green) and MAP2 (blue). Scale bar = 50 µm. (*B*) Quantification of integrated ankyrin G fluorescence intensity in neurons cultured in the presence of $CaCl_2$ (+2 or +5 mM), ATP (+1 mM), 100 nM BBG or EGTA (1–2 mM) and their corresponding combined treatments. (*C*) Sodium channel expression at the AIS of hippocampal neurons treated with 1 mM ATP and 2 mM EGTA. Neurons were stained with anti-PanNaCh antibody (green) and MAP2 (blue). Scale bar = 20 µm. (*D*) Quantification of integrated ankyrin G fluorescence intensity in neurons nucleofected with GFP, P2X7-GFP, scrambled shRNA, or P2X7 shRNA and treated with 2 mM EGTA or 2 mM $CaCl_2$. (*E*) Hippocampal neurons nucleofected with P2X7-GFP, cultured for 20 DIV and treated with 2 mM EGTA for 24 h. Neurons were fixed and stained with anti-PanNaCh antibody. The ×4 magnification of non-nucleofected and P2X7-GFP nucleofected neurons identified by letters are shown in the corresponding bottom panels. Scale bar = 50 µm. (*F*) Quantification of integrated sodium channel fluorescence intensity in neurons treated with 1 mM ATP or 2 mM $CaCl_2$ alone or in combination with 2 mM EGTA or 100 nM BBG, respectively. (*G*) Quantification of integrated sodium channel fluorescence intensity in control or 2 mM EGTA treated neurons nucleofected with GFP or P2X7-GFP. (**$P < 0.01$; ***$P < 0.001$, Mann–Whitney test).

allowing reperfusion. In 2 independent set of experiments, rats were separated in 2 groups that were treated intraperitoneally with BBG or vehicle after 3 and 6 h following reperfusion, and then twice a day. A third group was sham-operated without ischemia induction. Motor neuroscore tests gave a score of 5 in sham-operated rats, while rats subjected to ischemia kept the initial score of 3 until 72 h. However, BBG treated rats recovered partially obtaining a score of 4 at 72 h ($P < 0.05$, *t*-test).

Our results show a significant reduction in the number of AIS identified by ankyrin G and βIV-spectrin staining in ischemic brain tissue (Fig. 8*A*,*C*) compared with contralateral nonischemic cortical region (36.3 ± 7.8%, ipsilateral vs. 100%, contralateral; $P < 0.001$, $n = 5$). However, when rats were treated with BBG (50 mg/kg), the number of AIS preserved and identifiable in the ischemia region by ankyrin G and βIV-spectrin staining was significantly increased (88.6 ± 5.9% vs. 36.3.7 ± 7.8% in vehicle treated rats; $P < 0.001$, $n = 5$) (Fig. 8*B*,*D*). P2X7 staining was not detected at the AIS, suggesting that P2X7 receptors in other neuronal structures regulate AIS structure.

In conclusion, our data demonstrate the involvement of P2X7 receptor activity in the regulation of voltage-gated sodium channels and structural protein density at the AIS, and suggest a major role of the purinergic system in physiological and pathological modulation of neuronal excitability.

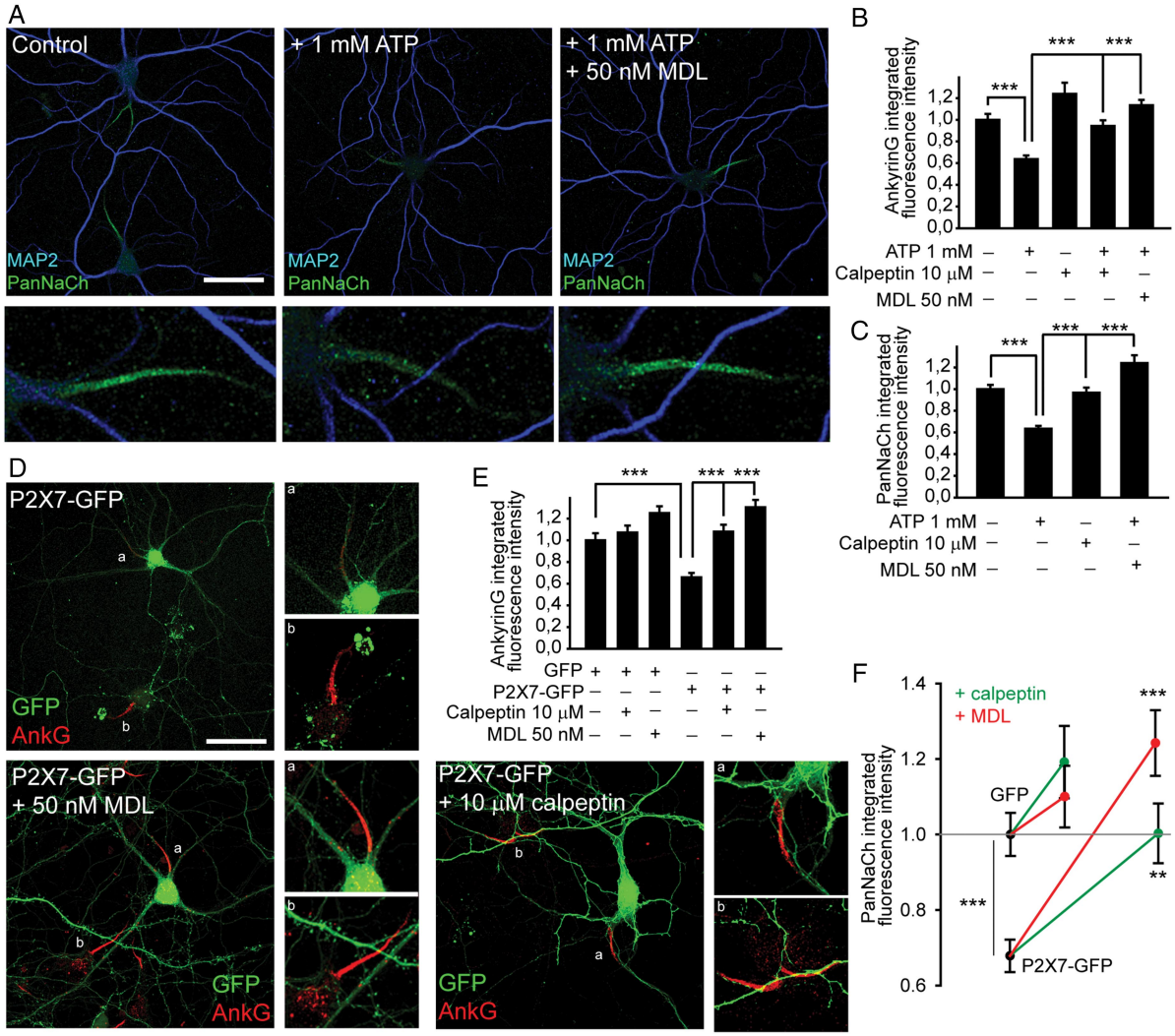

Figure 5. Calpain inhibition impairs the reduction of AIS protein density mediated by P2X7 receptors. (*A*) 20 DIV hippocampal neurons treated for the last 24 h with 1 mM ATP alone or in combination with the calpain inhibitor MDL-28170 (50 nM). Neurons were fixed and stained with anti-PanNaCh (green) and anti-MAP2 (blue) antibodies. Bottom panels show a ×4 magnification of AISs. (*B*,*C*) Quantification of integrated ankyrin G and sodium channels fluorescence intensity in neurons treated with 1 mM ATP alone or in combination with 10 μM calpeptin or 50 nM MDL. (*D*) 20 DIV hippocampal neurons nucleofected with P2X7-GFP plasmid and treated with the calpain inhibitors MDL (50 nM) or calpeptin (10 μM). Neurons were stained with antiankyrin G antibody (red). The ×4 magnifications show AISs from control nonnucleofected and P2X7-GFP nucleofected neurons. (*E*,*F*) Quantification of integrated ankyrin G and sodium channel fluorescence intensity in neurons nucleofected with GFP or P2X7-GFP plasmids and treated for 24 h with calpain inhibitors, MDL, or calpeptin. (**$P < 0.01$; ***$P < 0.001$, Mann–Whitney test).

Discussion

Ion channel modifications and mutations in the AIS have been related to a variety of brain diseases (for a review see, (Buffington and Rasband 2011). Our study demonstrates a new role for P2X7 receptors in the regulation and maintenance of the structural and functional properties of the AIS. P2X7 inhibition not only prevents AIS disruption after MCAO-induced brain ischemia, but also enhances neuronal excitability in cultured brain slices. In fact, ATP-mediated P2X7 activation or its exogenous receptor expression diminishes βIV-spectrin, ankyrin G and voltage-gated sodium channel expression at the AIS in brain slices or cultured hippocampal neurons. This occurs through calcium/calpain-mediated degradation, reducing sodium current amplitude and the number of action potentials. We show that P2X7 receptor is not detectable in the AIS, suggesting that mechanisms outside the AIS may regulate protein expression at the AIS. Furthermore, these results indicate a new major role of the purinergic system in the functional regulation of the AIS in physiological and pathological conditions.

P2X7 Modulation of AIS Function

Brain injury and neurodegenerative disorders are generally due to perturbations in the regulation of glial cells and/or neurons. P2X7 receptors are widely expressed in non-neuronal cells and neurons, and we cannot exclude the participation of non-neuronal P2X7 receptors in more complex models where glial cells are in closed contact with neurons. However, our data using a model of pure cultured neurons, where supporting glial cells are not in contact, point to a role of neuronal P2X7 receptor activation by ATP in the loss of AIS proteins. In fact, oxygen/glucose deprivation in cultured cortical or hippocampal neurons, in the absence of glial cells, results in the loss of AIS protein staining (Schafer et al. 2009) and this happens within the first 2 h before cell death. In our study, stimulation

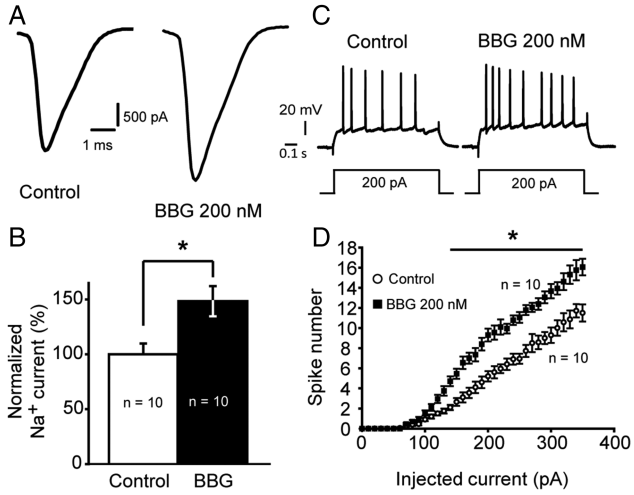

Figure 6. Inhibition of P2X7 receptors by BBG increases sodium current amplitude and intrinsic neuronal excitability. (*A*) Plot of the sodium current in CA3 hippocampal neurons from control or 200 nM BBG treated slices (350 μm). Sodium currents measured in CA3 hippocampal neurons were evoked by a depolarizing step from −70 to 0 mV. (*B*) Mean ± SEM normalized sodium current amplitude in 200 nM BBG treated neurons compared with control neurons. (*$P < 0.02$; paired *t*-test). Note the significant increase in the sodium current amplitude in BBG treated neurons. (*C*) Representative firing profiles of CA3 hippocampal neurons from control and 200 nM BBG treated slices. (*D*) Input–output curves for control (○) and BBG (●) treated neurons. Note the significant increase in excitability for BBG treated neurons (*t*-test, *$P < 0.02$).

of P2X7 receptor by ATP diminished the concentration of proteins at the AIS. In contrast, the AIS was still faintly detectable, suggesting that P2X7 receptor exerts a regulatory mechanism that controls the density of AIS proteins without completely disrupting AIS structure. In fact, P2X7 suppression impaired this reduction and even increased sodium channel density, as observed when P2X7 receptor was inhibited by BBG. Moreover, after prolonged ATP treatment, P2X7 inhibition rescued the density of AIS proteins, suggesting that there is a physiological turnover of AIS proteins. Thus, final concentration of some proteins at the AIS may depend on the equilibrium between calpain degradation and membrane insertion at the AIS of proteins from a reserve pool. This hypothesis may explain why P2X7 inhibition with BBG increases AIS proteins density. Further experiments will be necessary to understand how AIS proteins density is regulated and their contribution to neuronal function. Hence, the P2X7 receptor has a physiological role in AIS regulation, besides its pathological role in ischemia that is probably coupled to other inflammatory mechanisms (Friedle et al. 2010). These changes in sodium channel expression were confirmed by our electrophysiological studies in neurons from organotypic slice cultures, containing the hippocampus and the cortex, where P2X7 exogenous expression in neurons reduced sodium current amplitude by 50% and diminished the expression of the scaffolding protein βIV-spectrin in the AIS. As mentioned above, P2X7 activity can trigger ATP release to the extracellular medium (Gutierrez-Martin et al. 2011), thus accounting for the reduction of AIS proteins density by exogeneous expression of P2X7-GFP. In contrast, BBG inhibition increased sodium current amplitude in the same range. Moreover, in both cases these changes in sodium current were reflected by the number of action potentials generated, corroborating the data obtained from cultured neurons.

A recent report has pointed out that micromolar concentrations of BBG may inactivate $Na_v1.3$ sodium channels in neuroblastoma cells (Jo and Bean 2011). We do not believe that this mechanism contributes to our data since BBG was used at lower concentrations (50–200 nM;, i.e., the range for specific inhibition of the P2X7 receptor (Jiang et al. 2000)). In addition, BBG actually increased sodium channel density, neuronal excitability and sodium currents. Furthermore, the concentration of BBG measured in mouse brain after repetitive intraperitoneal injections of BBG never exceeds 200 nM (Diaz-Hernandez et al. 2012).

What is the mechanism of P2X7-dependent regulation of AIS structure? Sustained activation of calpain has been described in neurodegenerative diseases, such as Parkinson's, Alzheimer's or Huntington's disease (for a review see, Vosler et al. 2008), and traumatic brain or spinal cord injury (Kampfl et al. 1996; Ray et al. 2003). Calcium (and subsequently calpain) disrupts the AIS cytoskeleton. This process is thought to account for the AIS dissipation observed in brain ischemia since it is prevented by the calpain inhibitor MDL-28170 (Schafer et al. 2009). Calpain is activated by increased intracellular calcium concentration. Our data show that the P2X7 receptor mediates the calcium influx at the origin of these alterations in the AIS. We cannot exclude that voltage-gated calcium channels have a minor contribution as they may be opened as a consequence of P2X7 activation. In fact, Brater et al. (1999) described in NG108-15 cells that 28% of ATP-induced calcium influx is blocked by the L-type calcium channels blocker, nifedipine. Recent evidences show that calcium influx through L-type voltage-gated calcium channels is involved in the modulation of another type of AIS plasticity, modulating AIS position or length (Grubb and Burrone 2010; Kuba et al. 2010). However, authors did not report any change in AIS proteins density, and our study shows that P2X7 mediated mechanisms do not change AIS position or length (Supplementary Fig. 1). Thus, our data suggest that ATP-mediated activation of P2X7 receptors control a different type of AIS plasticity in response to different stimulus. Even more, calcium mediated modulation of AIS position do not depend on calpain, but instead needs calcineurin activation (Evans et al. 2013). In fact, we show that calcium-dependent alterations in the AIS were abolished by calpain inhibitors, P2X7 receptor inhibition or P2X7 knockdown. Reciprocally, extracellular calcium depletion impaired the reduction in AIS protein density induced by ATP or P2X7-GFP expression. Moreover, it has been reported that P2X7 activation by ATP induces calpain-dependent protein cleavage in cortical neurons and Par C5 cells (Hwang et al. 2009; Nishida et al. 2012). Furthermore, recent studies have shown that βIV-spectrin, ankyrin G, and voltage-gated sodium channels are substrates for calpain (Schafer et al. 2009; von Reyn et al. 2009). This may account for the reduction of βIV-spectrin, ankyrin G ,and sodium channels at the AIS observed in our study, and its recovery by calpain inhibitors, P2X7 antagonist or P2X7 interference RNA.

P2X7 Involvement in AIS Disruption During Brain Ischemia

Due to the role of AIS in neuronal excitability, physiological and pathological modifications in its organization are expected to generate neurological disorders. Multiple nonsynonymous single nucleotide polymorphisms (NS-SNPs) have been identified in the

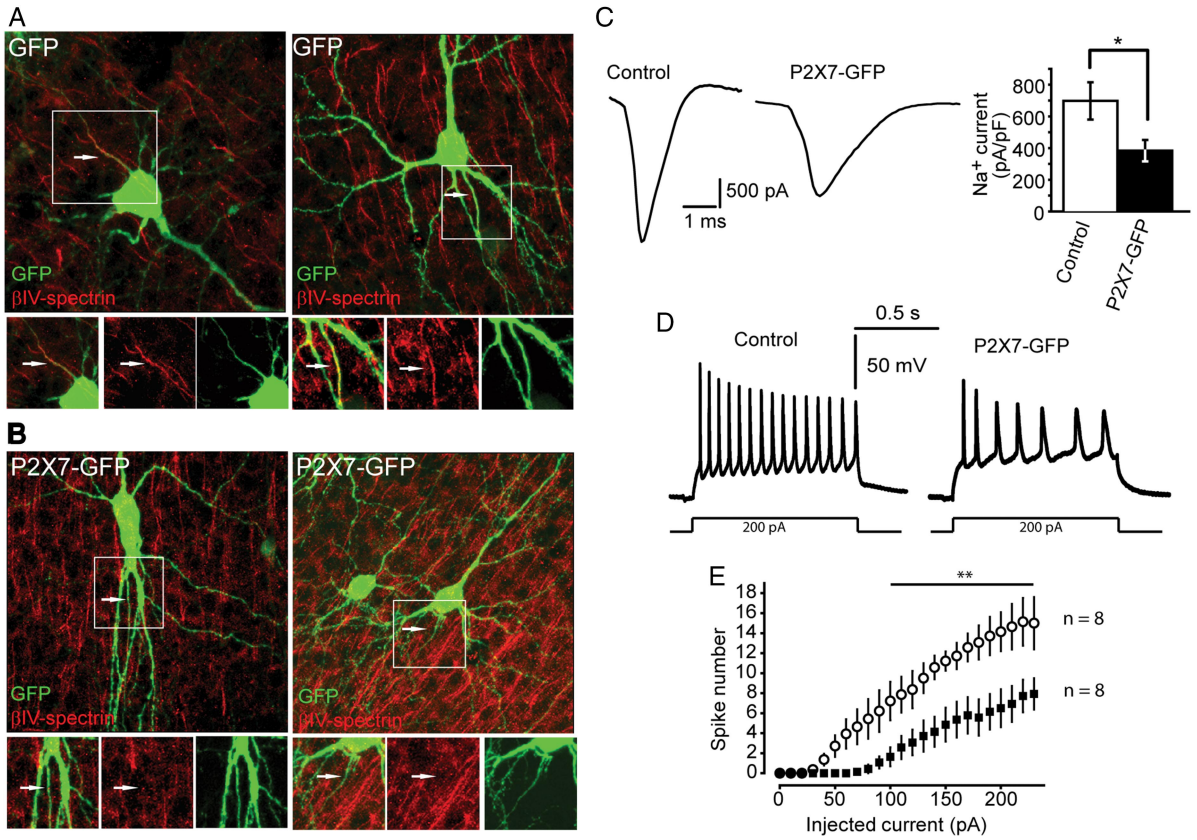

Figure 7. Expression of P2X7-GFP receptors in cortical neurons diminishes sodium current amplitude, intrinsic excitability, and βIV-spectrin density at the AIS. (*A*,*B*) GFP (A) or P2X7-GFP (B) expression plasmids were transfected in 450 μm brain slices including hippocampus and entorhinal cortex using the biolistic technique GeneGun. Brain slices were fixed and stained using an antibody against the AIS marker βIV-spectrin (red). Images show layer V cortical neurons. Note that the AIS of neurons expressing GFP show clear βIV-spectrin staining similar to that of surrounding GFP negative neurons, while βIV-spectrin staining is absent from the AIS of P2X7-GFP positive neurons. (*C*) Plot of the sodium current in L5 cortical neurons from control (GFP) or P2X7-GFP positive neurons. Sodium currents were evoked by a depolarizing step from −70 to 0 mV. The graph represents the mean ± SEM of the sodium current amplitude measured in control or P2X7-GFP neurons ($n = 8$; $^*P < 0.05$; *t*-test). Note the significant reduction in the sodium current amplitude in P2X7-GFP positive neurons. (*D*) Representative firing profiles of L5 cortical neurons from control and P2X7-GFP neurons. (*E*) Input–output curves for control (○) and P2X7-GFP positive neurons (●). Note the significant neuronal excitability decrease in P2X7-GFP neurons (*t*-test, $^*P < 0.01$).

human P2X7 gene, which generate different mutant P2X7 receptors. Most of these mutations engender modifications in calcium permeability and are associated with diseases, including bipolar disorder, major depressive disorder, anxiety disorders, multiple sclerosis, ischemic stroke, and neuropathic pain (Jiang et al. 2013). Our results demonstrate a role of the P2X7 purinergic receptor in the damage suffered by the AIS after ischemia/reperfusion, and protection by the P2X7 antagonist, BBG, when applied in the first 3 h after ischemia induction. In this sense, it is noteworthy that 17β-oestradiol, a natural protector against ischemic injury (Perez-Alvarez et al. 2012) inhibits P2X7 receptor activity (Cario-Toumaniantz et al. 1998). Interestingly, BBG treatment after ischemia exerts a neuroprotective effect and moderately reduces both neuronal death (Arbeloa et al. 2012), and brain edema after traumatic brain injury (Kimbler et al. 2012). A previous study has shown that the AIS is disrupted before cell death when brain ischemia is induced by MCAO (Schafer et al. 2009), leading to a loss of structural and functional proteins (βIV-spectrin, ankyrin G and voltage-gated ion channels). In contrast to our study, this was not prevented by the inhibition of calcium-permeable NMDA receptors using MK-801, which in turn can increase neuronal survival after oxygen/glucose deprivation (Schafer et al. 2009). While it has been shown that P2X7 receptor levels measured by immunoblot do not change after traumatic brain injury (Kimbler et al. 2012), this receptor exhibits an increased response to ATP after ischemic insult (Wirkner et al. 2005), even in the absence of an increment in P2X7 expression. However, other studies demonstrate up-regulation of P2X7 mRNA in neurons after focal cerebral ischemia (Cavaliere et al. 2004; Franke et al. 2004). In agreement with these studies our experiments indicated that the increased P2X7 receptor density induced by exogenous expression in brain slices is sufficient to disrupt AIS integrity. Moreover, the extracellular concentration of the P2X7 receptor agonist ATP is highly augmented after MCAO (Melani et al. 2005) or spinal cord injury (Wang et al. 2004). Reciprocally, ATP injection increases brain damage after ischemia (Zhang et al. 2013), while ATP depletion by ectonucleotidases may play a role in protection against brain damage after ischemia (Melani et al. 2012). Hence, an increase in either extracellular ATP or P2X7 receptor expression mediates the harmful processes activated during brain ischemia. In view of these results, P2X7 receptors seem to be a major source of calcium influx involved in AIS disruption after brain ischemia, and also a good candidate to modulate AIS function in certain physiological conditions.

In conclusion, our results support a role for the P2X7 purinergic receptor in the modulation of protein density at the AIS and neuronal excitability. As different levels of ATP and other

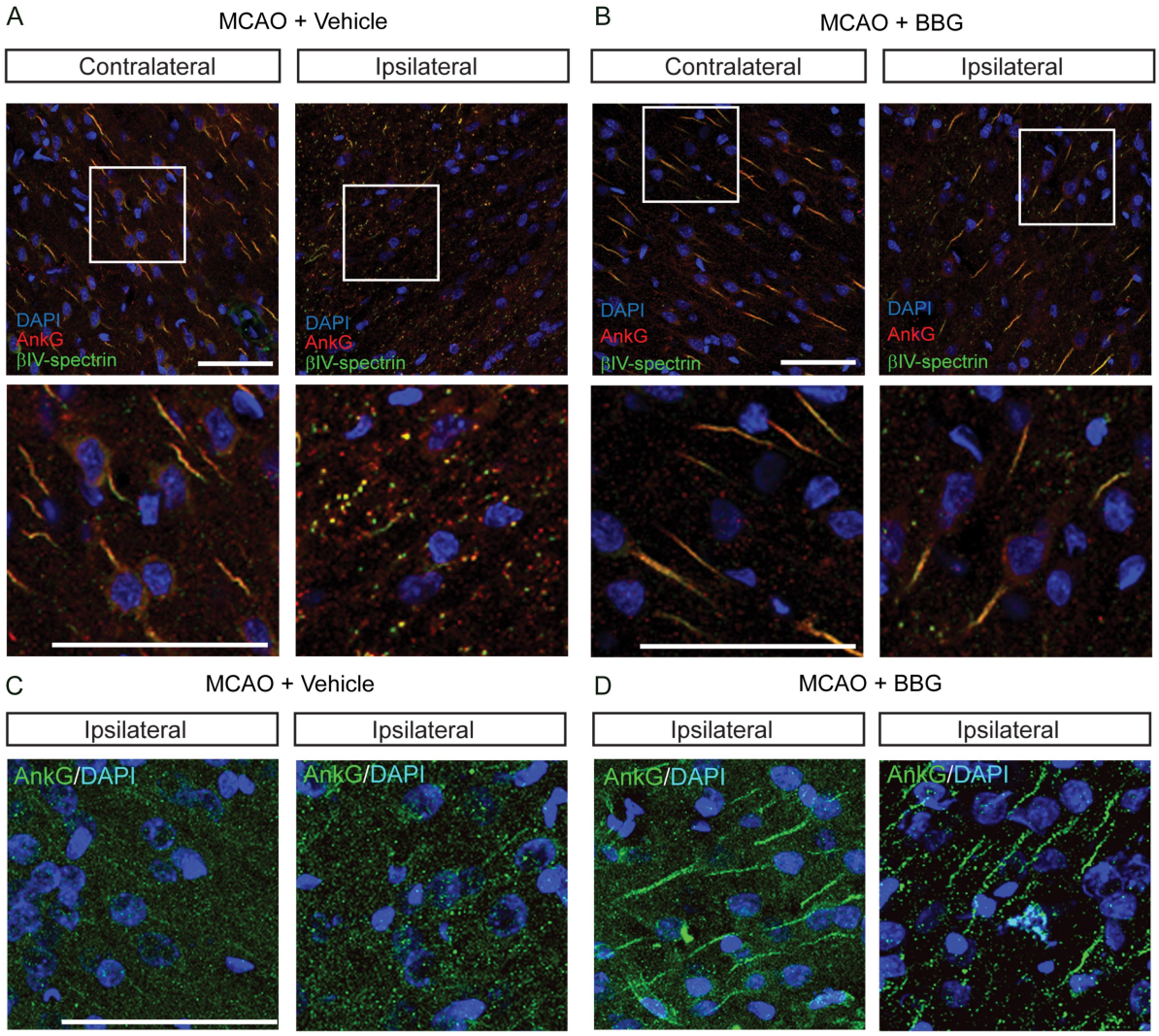

Figure 8. A P2X7 receptor antagonist prevents AIS injury in ischemia. (*A*,*B*) Rats were operated to induce brain ischemia by middle cerebral artery occlusion (MCAO). Rats were injected intraperitoneally with PBS or the P2X7 receptor antagonist BBG (50 mg/kg) as described in Materials and Methods section. Brains were collected 72 h later. Coronal sections (30 μm) were stained with antiankyrin G (red) and antiβIV-spectrin (green) antibodies. Nuclei were stained using 4′,6-diamidino-2-phenylindole (blue). Images show representative pictures from the parietal cortex region of the contralateral side (undamaged region) or ipsilateral side (ischemic zone) from rat brains treated with vehicle (PBS) or BBG. White square zones were magnified 3 times and shown in the corresponding bottom panels. (*C*,*D*) Images from regions of ischemia damage from rat brains of a second independent experiment showing the absence of ankyrin G staining (green) in vehicle treated rats (*C*) and its protection in BBG treated rats (*D*). Scale bar = 50 μm.

related purines are released into the extracellular medium in different physiological as well as pathological conditions, it is tempting to propose that other purinergic receptors, such as P2Y receptors, and purines can also contribute to AIS modulation. In fact, a selective agonist of the P2Y1 receptor, 2-MeSADP, have been identified as a neuroprotective agent in a photothrombosis model of brain ischemia (Zheng et al. 2010). Finally, further experiments are necessary to understand how the activity of P2X7 receptors and calpain are finely regulated during structural modulation of the AIS, as well as the possible participation of non-neuronal cells in the regulation of AIS function by the purinergic system.

Supplementary Material

Supplementary material can be found at: http://www.cercor.oxfordjournals.org/.

Funding

This work was supported by grants SAF2009-12249-C02-02 and SAF2009-12249-C02-01 and SAF-SAF2012-39148-C03-03 from Plan Nacional I+D+i (Spain), INSERM and Agence National de la Recherche (EXCION, EPISOM). Ana del Puerto is supported by an FPI grant from Universidad Autónoma de Madrid.

Notes

The authors acknowledge Dr Michael Seagar for critical reading of the manuscript, Dr Matthew Rasband for supplying the βIV-spectrin antibody used in this study and Mónica Tapia and Diana Sanchez-Ponce from J.J.G. laboratory for their help and comments. We want to thank also the IMéRA (L'Institut Méditerranéen de Recherches Avancées), Aix-Marseille Université and INSERM (France) for the support given to J.J.G. *Conflict of Interest*: None declared.

References

Abbracchio MP, Burnstock G, Verkhratsky A, Zimmermann H. 2009. Purinergic signalling in the nervous system: an overview. Trends Neurosci. 32:19–29.

Arbeloa J, Perez-Samartin A, Gottlieb M, Matute C. 2012. P2X7 receptor blockade prevents ATP excitotoxicity in neurons and reduces brain damage after ischemia. Neurobiol Dis. 45:954–961.

Baalman KL, Cotton RJ, Rasband SN, Rasband MN. 2013. Blast wave exposure impairs memory and decreases axon initial segment length. J Neurotrauma. 30:741–751.

Bender KJ, Trussell LO. 2012. The physiology of the axon initial segment. Annu Rev Neurosci. 35:249–265.

Brater M, Li SN, Gorodezkaya IJ, Andreas K, Ravens U. 1999. Voltage-sensitive Ca^{2+} channels, intracellular Ca^{2+} stores and Ca^{2+}-release-activated Ca^{2+} channels contribute to the ATP-induced $[Ca^{2+}]i$ increase in differentiated neuroblastoma × glioma NG 108–15 cells. Neurosci Lett. 264:97–100.

Brechet A, Fache MP, Brachet A, Ferracci G, Baude A, Irondelle M, Pereira S, Leterrier C, Dargent B. 2008. Protein kinase CK2 contributes to the organization of sodium channels in axonal membranes by regulating their interactions with ankyrin G. J Cell Biol. 183:1101–1114.

Buffington SA, Rasband MN. 2011. The axon initial segment in nervous system disease and injury. Eur J Neurosci. 34:1609–1619.

Cario-Toumaniantz C, Loirand G, Ferrier L, Pacaud P. 1998. Non-genomic inhibition of human P2X7 purinoceptor by 17beta-oestradiol. J Physiol. 508(Pt 3):659–666.

Cavaliere F, Amadio S, Sancesario G, Bernardi G, Volonte C. 2004. Synaptic P2X7 and oxygen/glucose deprivation in organotypic hippocampal cultures. J Cereb Blood Flow Metab. 24:392–398.

Cruz DA, Weaver CL, Lovallo EM, Melchitzky DS, Lewis DA. 2009. Selective alterations in postsynaptic markers of chandelier cell inputs to cortical pyramidal neurons in subjects with schizophrenia. Neuropsychopharmacology. 34:2112–2124.

Debanne D, Boudkkazi S, Campanac E, Cudmore RH, Giraud P, Fronzaroli-Molinieres L, Carlier E, Caillard O. 2008. Paired-recordings from synaptically coupled cortical and hippocampal neurons in acute and cultured brain slices. Nat Protoc. 3:1559–1568.

del Puerto A, Diaz-Hernandez JI, Tapia M, Gomez-Villafuertes R, Benitez MJ, Zhang J, Miras-Portugal MT, Wandosell F, Diaz-Hernandez M, Garrido JJ. 2012. Adenylate cyclase 5 coordinates the action of ADP, P2Y1, P2Y13 and ATP-gated P2X7 receptors on axonal elongation. J Cell Sci. 125:176–188.

Diaz-Hernandez JI, Gomez-Villafuertes R, Leon-Otegui M, Hontecillas-Prieto L, Del Puerto A, Trejo JL, Lucas JJ, Garrido JJ, Gualix J, Miras-Portugal MT et al. 2012. In vivo P2X7 inhibition reduces amyloid plaques in Alzheimer's disease through GSK3beta and secretases. Neurobiol Aging. 33:1816–1828.

Diaz-Hernandez M, del Puerto A, Diaz-Hernandez JI, Diez-Zaera M, Lucas JJ, Garrido JJ, Miras-Portugal MT. 2008. Inhibition of the ATP-gated P2X7 receptor promotes axonal growth and branching in cultured hippocampal neurons. J Cell Sci. 121:3717–3728.

Diaz-Hernandez M, Diez-Zaera M, Sanchez-Nogueiro J, Gomez-Villafuertes R, Canals JM, Alberch J, Miras-Portugal MT, Lucas JJ. 2009. Altered P2X7-receptor level and function in mouse models of Huntington's disease and therapeutic efficacy of antagonist administration. FASEB J. 23:1893–1906.

Ehrengruber MU, Hennou S, Bueler H, Naim HY, Deglon N, Lundstrom K. 2001. Gene transfer into neurons from hippocampal slices: comparison of recombinant Semliki Forest Virus, adenovirus, adeno-associated virus, lentivirus, and measles virus. Mol Cell Neurosci. 17:855–871.

Evans MD, Sammons RP, Lebron S, Dumitrescu AS, Watkins TB, Uebele VN, Renger JJ, Grubb MS. 2013. Calcineurin signaling mediates activity-dependent relocation of the axon initial segment. J Neurosci. 33:6950–6963.

Franke H, Gunther A, Grosche J, Schmidt R, Rossner S, Reinhardt R, Faber-Zuschratter H, Schneider D, Illes P. 2004. P2X7 receptor expression after ischemia in the cerebral cortex of rats. J Neuropathol Exp Neurol. 63:686–699.

Friedle SA, Curet MA, Watters JJ. 2010. Recent patents on novel P2X(7) receptor antagonists and their potential for reducing central nervous system inflammation. Recent Pat CNS Drug Discov. 5:35–45.

Garrido JJ, Giraud P, Carlier E, Fernandes F, Moussif A, Fache MP, Debanne D, Dargent B. 2003. A targeting motif involved in sodium channel clustering at the axonal initial segment. Science. 300:2091–2094.

Grubb MS, Burrone J. 2010. Activity-dependent relocation of the axon initial segment fine-tunes neuronal excitability. Nature. 465:1070–1074.

Gutierrez-Martin Y, Bustillo D, Gomez-Villafuertes R, Sanchez-Nogueiro J, Torregrosa-Hetland C, Binz T, Gutierrez LM, Miras-Portugal MT, Artalejo AR. 2011. P2X7 receptors trigger ATP exocytosis and modify secretory vesicle dynamics in neuroblastoma cells. J Biol Chem. 286:11370–11381.

Hedstrom KL, Ogawa Y, Rasband MN. 2008. AnkyrinG is required for maintenance of the axon initial segment and neuronal polarity. J Cell Biol. 183:635–640.

Hinman JD, Rasband MN, Carmichael ST. 2013. Remodeling of the axon initial segment after focal cortical and white matter stroke. Stroke. 44:182–189.

Hwang SM, Li J, Koo NY, Choi SY, Lee SJ, Oh SB, Castro R, Kim JS, Park K. 2009. Role of purinergic receptor in alpha fodrin degradation in Par C5 cells. J Dent Res. 88:927–932.

Jiang LH, Baldwin JM, Roger S, Baldwin SA. 2013. Insights into the molecular mechanisms underlying mammalian P2X7 receptor functions and contributions in diseases, revealed by structural modeling and single nucleotide polymorphisms. Front Pharmacol. 4:55.

Jiang LH, Mackenzie AB, North RA, Surprenant A. 2000. Brilliant blue G selectively blocks ATP-gated rat P2X(7) receptors. Mol Pharmacol. 58:82–88.

Jo S, Bean BP. 2011. Inhibition of neuronal voltage-gated sodium channels by brilliant blue G. Mol Pharmacol. 80:247–257.

Kaech S, Banker G. 2006. Culturing hippocampal neurons. Nat Protoc. 1:2406–2415.

Kampfl A, Posmantur R, Nixon R, Grynspan F, Zhao X, Liu SJ, Newcomb JK, Clifton GL, Hayes RL. 1996. Mu-calpain activation and calpain-mediated cytoskeletal proteolysis following traumatic brain injury. J Neurochem. 67:1575–1583.

Kaphzan H, Buffington SA, Jung JI, Rasband MN, Klann E. 2011. Alterations in intrinsic membrane properties and the axon initial segment in a mouse model of Angelman syndrome. J Neurosci. 31:17637–17648.

Kim JE, Kwak SE, Jo SM, Kang TC. 2009. Blockade of P2X receptor prevents astroglial death in the dentate gyrus following pilocarpine-induced status epilepticus. Neurol Res. 31:982–988.

Kimbler DE, Shields J, Yanasak N, Vender JR, Dhandapani KM. 2012. Activation of P2X7 promotes cerebral edema and neurological injury after traumatic brain injury in mice. PLoS One. 7:e41229.

Kole MH, Ilschner SU, Kampa BM, Williams SR, Ruben PC, Stuart GJ. 2008. Action potential generation requires a high sodium channel density in the axon initial segment. Nat Neurosci. 11:178–186.

Kuba H, Oichi Y, Ohmori H. 2010. Presynaptic activity regulates Na(+) channel distribution at the axon initial segment. Nature. 465:1075–1078.

Longa EZ, Weinstein PR, Carlson S, Cummins R. 1989. Reversible middle cerebral artery occlusion without craniectomy in rats. Stroke. 20:84–91.

Matute C, Torre I, Perez-Cerda F, Perez-Samartin A, Alberdi E, Etxebarria E, Arranz AM, Ravid R, Rodriguez-Antiguedad A, Sanchez-Gomez M et al. 2007. P2X(7) receptor blockade prevents ATP excitotoxicity in oligodendrocytes and ameliorates experimental autoimmune encephalomyelitis. J Neurosci. 27:9525–9533.

Melani A, Corti F, Stephan H, Muller CE, Donati C, Bruni P, Vannucchi MG, Pedata F. 2012. Ecto-ATPase inhibition: ATP and adenosine release under physiological and ischemic in vivo conditions in the rat striatum. Exp Neurol. 233:193–204.

Melani A, Turchi D, Vannucchi MG, Cipriani S, Gianfriddo M, Pedata F. 2005. ATP extracellular concentrations are increased in the rat striatum during in vivo ischemia. Neurochem Int. 47:442–448.

Nishida K, Nakatani T, Ohishi A, Okuda H, Higashi Y, Matsuo T, Fujimoto S, Nagasawa K. 2012. Mitochondrial dysfunction is involved in P2X7 receptor-mediated neuronal cell death. J Neurochem. 122:1118–1128.
North RA, Surprenant A. 2000. Pharmacology of cloned P2X receptors. Annu Rev Pharmacol Toxicol. 40:563–580.
Ogawa Y, Horresh I, Trimmer JS, Bredt DS, Peles E, Rasband MN. 2008. Postsynaptic density-93 clusters Kv1 channels at axon initial segments independently of Caspr2. J Neurosci. 28:5731–5739.
Pan Z, Kao T, Horvath Z, Lemos J, Sul JY, Cranstoun SD, Bennett V, Scherer SS, Cooper EC. 2006. A common ankyrin-G-based mechanism retains KCNQ and NaV channels at electrically active domains of the axon. J Neurosci. 26:2599–2613.
Parvathenani LK, Tertyshnikova S, Greco CR, Roberts SB, Robertson B, Posmantur R. 2003. P2X7 mediates superoxide production in primary microglia and is up-regulated in a transgenic mouse model of Alzheimer's disease. J Biol Chem. 278:13309–13317.
Perez-Alvarez MJ, Maza Mdel C, Anton M, Ordonez L, Wandosell F. 2012. Post-ischemic estradiol treatment reduced glial response and triggers distinct cortical and hippocampal signaling in a rat model of cerebral ischemia. J Neuroinflammation. 9:157.
Ray SK, Hogan EL, Banik NL. 2003. Calpain in the pathophysiology of spinal cord injury: neuroprotection with calpain inhibitors. Brain Res Brain Res Rev. 42:169–185.
Sanchez-Ponce D, Munoz A, Garrido JJ. 2011. Casein kinase 2 and microtubules control axon initial segment formation. Mol Cell Neurosci. 46:222–234.
Schafer DP, Jha S, Liu F, Akella T, McCullough LD, Rasband MN. 2009. Disruption of the axon initial segment cytoskeleton is a new mechanism for neuronal injury. J Neurosci. 29:13242–13254.
Tapia M, Del Puerto A, Puime A, Sanchez-Ponce D, Fronzaroli-Molinieres L, Pallas-Bazarra N, Carlier E, Giraud P, Debanne D, Wandosell F et al. 2013. GSK3 and beta-catenin determines functional expression of sodium channels at the axon initial segment. Cell Mol Life Sci. 70:105–120.
Vacher H, Yang JW, Cerda O, Autillo-Touati A, Dargent B, Trimmer JS. 2011. Cdk-mediated phosphorylation of the Kvbeta2 auxiliary subunit regulates Kv1 channel axonal targeting. J Cell Biol. 192:813–824.
Vianna EP, Ferreira AT, Naffah-Mazzacoratti MG, Sanabria ER, Funke M, Cavalheiro EA, Fernandes MJ. 2002. Evidence that ATP participates in the pathophysiology of pilocarpine-induced temporal lobe epilepsy: fluorimetric, immunohistochemical, and Western blot studies. Epilepsia 43(Suppl 5):227–229.
von Reyn CR, Spaethling JM, Mesfin MN, Ma M, Neumar RW, Smith DH, Siman R, Meaney DF. 2009. Calpain mediates proteolysis of the voltage-gated sodium channel alpha-subunit. J Neurosci. 29: 10350–10356.
Vosler PS, Brennan CS, Chen J. 2008. Calpain-mediated signaling mechanisms in neuronal injury and neurodegeneration. Mol Neurobiol. 38:78–100.
Wang X, Arcuino G, Takano T, Lin J, Peng WG, Wan P, Li P, Xu Q, Liu QS, Goldman SA et al. 2004. P2X7 receptor inhibition improves recovery after spinal cord injury. Nat Med. 10:821–827.
Wirkner K, Kofalvi A, Fischer W, Gunther A, Franke H, Groger-Arndt H, Norenberg W, Madarasz E, Vizi ES, Schneider D et al. 2005. Supersensitivity of P2X receptors in cerebrocortical cell cultures after in vitro ischemia. J Neurochem. 95:1421–1437.
Yrjanheikki J, Koistinaho J, Kettunen M, Kauppinen RA, Appel K, Hull M, Fiebich BL. 2005. Long-term protective effect of atorvastatin in permanent focal cerebral ischemia. Brain Res. 1052:174–179.
Zhang M, Li W, Niu G, Leak RK, Chen J, Zhang F. 2013. ATP induces mild hypothermia in rats but has a strikingly detrimental impact on focal cerebral ischemia. J Cereb Blood Flow Metab. 33:1–10.
Zheng W, Watts LT, Holstein DM, Prajapati SI, Keller C, Grass EH, Walter CA, Lechleiter JD. 2010. Purinergic receptor stimulation reduces cytotoxic edema and brain infarcts in mouse induced by photothrombosis by energizing glial mitochondria. PLoS One. 5: e14401.